KKU Res. J. 2013; 18(2): 191-199
http : //resjournal.kku.ac.th

Combined Convective and Radiative Heat Transfer on Transpiration Cooling System in Al–Co Open–celled Foam having PPI of 20

Pipatana Amatachaya[1] *Bundit Krittacom*[1,*] *and Rapeepong Peamsuwan*[2]

[1] *Development In Technology Of Porous Materials Research Laboratory (DITO-Lab), Department of Mechanical Engineering, Faculty of Engineering and Architecture,*
[2] *Department of Applied Physics, Faculty of Sciences and Liberal Arts, Rajamangala University of Technology Isan (RMUTI), 744 Suranarai Road, Maung, Nakhonratchasima, 30000, THAILAND, Tel: +664-423-3073, Fax: +664-423-3074*
* *Correspondent author: bundit.kr@rmuti.ac.th and bundit_krittacom@hotmail.com*

Abstract

One-dimensional transpiration cooling system in open-celled foam has been conducted experimentally and numerically to investigate the heat transfer characteristics of combined convection and radiation. The Alumina–Cordierite (Al-Co) open-cell foam having porosity of 0.875 and pores per inch (PPI) of 20 was employed. The upper surface of porous plate was heated by the heat flux of incoming radiation ($q_{Rx,f}$) varying from 0.97 - 16.59 kW/m^2 whereas air injection velocity (u_f) fed into the lower surface was varied from 0.364 - 1.274 m/s, and was then rearranged as Reynolds number (Re). For the report of the results in the present study, two efficiencies including of temperature (η_T) and conversion efficiency (η_C) were presented. The η_T increased rapidly with the air injection velocity (Re). It was then saturated and had a constant value at Re higher than 15. For the result of η_C, it was decreased slightly with increasing of $q_{Rx,f}$ and u_f (Re). The numerical predictions also agreed with experimental data very well.

Keywords: Open-cell foam, Radiation, Transpiration cooling, Reynolds number

1. Introduction

Transpiration cooling or effusion cooling (1) is the process of injecting a fluid (Air) into a porous material which can be served as a very efficient cooling method for protecting solid surfaces that are exposed to high-heat-flux, high-temperature from environments such as in hypersonic vehicle combustors, rocket nozzle, gas turbine blades, and the structure of re-entry aerospace vehicles (1–5). The performance of this cooling system is governed by several parameters such as radiative properties of porous media, the volumetric heat transfer coefficient between the solid phase and fluid, fluid velocity and irradiation. Thus, the knowledge of parameters for the design of transpiration-cooled devices is classified into two main groups including the phenomena of fluid flow and heat transfer process within the porous plate.

So far a number of experimental works (6–8) and numerical studies (9–12) have been conducted on transpiration cooling system. However, most of previous studies were mainly intended to determine the effects of convection mode. There were only a few studies have taken into account the radiative heat transfer in the transpiration cooling system. Recently, Jiang et al. (13) and Kamiuto et al. (14) investigated experimentally and analytically to extend the validation of numerical model. Jiang et al. (13) found that the numerical results corresponded well with the experimental data including the surface temperature and heat transfer coefficients. However, their work still focused on the effects of convective heat transfer. Radiation mode was concerned in the investigation of Kamiuto et al. (14). They reported that the agreement between theoretical prediction and experimental results was acceptable. Although Kamiuto and co-worker (14) regarded the radiation mode in the transpiration cooling system, the theoretical result was more emphasized and there exist the difference between theory and experiment.

Based on the work of Kamiuto et al. (14), the present research aims to further experiment and analyze the heat transfer phenomena as combined convection and radiation in the transpiration cooling system using open-cellular porous material. Alumina-Cordierite (Al-Co) having PPI of 20 is adopted owing to this Al-Co has a higher porosity resulting to a higher efficient of heat transfer and is widely used as thermal insulation of industry (15). Obtainable quantities such as temperature at the surfaces and within the porous plate, for theoretical results, are presented and comparison with experimental data is also reported. A tip for design is recommended.

2. Nomenclature

$C_{f,}$ isobaric specific heat capacity ($J \cdot kg^{-1} \cdot K^{-1}$)

D_C a normal cell diameter (m)

D_P equivalent strut diameter (m)

$\tilde{g}$ asymmetric factor of scattering phase function

G incident radiation (W/m^2)

h_v volumetric heat transfer coefficient between gas and solid phases ($W \cdot m^{-3} \cdot K^{-1}$)

k_f thermal conductivity of a gas phase ($W \cdot m^{-2} \cdot K^{-1}$)

k_s thermal conductivity of a solid phase ($W \cdot m^{-2} \cdot K^{-1}$)

q_{Rx} net radiative heat flux in x direction (W/m^2)

T_f temperature of a gas phase (^oC)

T_R radiation blackbody temperature (K)

T_s temperature of a solid phase (^oC)

T_∞ ambient temperature (K)

u_f air flow velocity (m/s)

w dimensionless width of a strut with a square cross section (m)

x coordinate in the flow direction (m)

Greek Symbols

β scaled extinction coefficient (m^{-1})

ϕ porosity

η_T temperature efficiency

η_C conversion efficiency

$\rho\phi$ density of a gas phase or air (kg/m^3)

σ Stefan–Boltzmann constant ($=5.67\times10^{-8}$ $W\bullet m^{-2}\bullet K^{-4}$)

τ optical thickness

ω scaled albedo

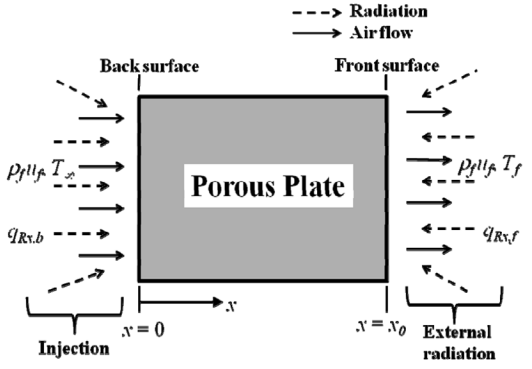

Figure 1. The theoretical model and coordinate of a transpiration cooling system.

3. Theoretical Analysis

3.1 Mathematical Model

The present model of a transpiration cooling system is shown in Fig. 1. The assumptions of the numerical model are similar to those of Kamiuto et al. (14). However, some modification was made to improve the accurate prediction. The following assumptions were introduced for this analysis as follows: 1) An open-cellular porous plate of thickness x_0 is placed horizontally; 2) The front surface of porous plate is uniformly irradiated by blackbody radiation at an equivalent temperature T_R (K), while the back surface is subject to uniform blackbody radiation at an inlet air temperature; 3) A low-temperature air is injected through the back surface of porous plate and is assumed to be non-radiating; 4) The porous medium is gray and is capable of emitting, absorbing and anisotropically scattering thermal radiation; 5) The porous medium is non-catalytic; 6) The physical properties depend on temperature differed from Kamiuto's work (14) that the physical properties of his work (14) did not depend on temperature; 7) The heat transfer within the porous plate is in an one-dimensional steady-state; 8) The behavior of air flow within porous plate is under local and non-thermal equilibrium condition.

Under these assumptions, the continuity equation is given by:

$$\frac{\partial\left(\rho_f u_f\right)}{\partial x}=0\,. \tag{1}$$

The governing energy equations for the gas and the solid phases (porous plate) may be written as follows:

$$\rho_f u_f C_f \frac{\partial T_f}{\partial x}=\phi\frac{\partial}{\partial x}\left(k_f\frac{\partial T_f}{\partial x}\right)-h_v\left(T_f-T_s\right), \tag{2}$$

$$\frac{1}{3}(1-\phi)\frac{\partial}{\partial x}\left(k_s\frac{\partial T_s}{\partial x}\right)+h_v\left(T_f-T_s\right)-\frac{\partial q_{Rx}}{\partial x}=0\,, \tag{3}$$

$$\frac{\partial q_{Rx}}{\partial x}=4\beta(1-\omega)\left(\sigma T_s^4-\frac{G}{4}\right), \tag{4}$$

Four physical properties, i.e., ϕ, β, h_v and ω from Eq. (2) to (4) were summarized by Krittacom (16) and were briefly recalled as following:

$$\beta=\frac{\pi}{4}\left[\left(\frac{6}{\pi}\right)^{2/3}w^2+\frac{4w}{\sqrt{\pi}}(1-w)\right]\times\frac{1}{D_C}(1-w) \tag{5}$$

$$D_c=\frac{0.0254}{PPI} \tag{6}$$

$$w = 0.5 + \cos\left[\frac{1}{3}\cos^{-1}\left(2\phi - 1\right) + \frac{4}{3}\pi\right] \quad (7)$$

$$\frac{h_v D_P^2}{k_f} = 0.124\left(\mathrm{Re}\,\mathrm{Pr}\right)^{0.792} \quad (8)$$

$$D_p = \frac{2wD_c}{\sqrt{\pi}} \quad (9)$$

$$\omega = 0.698 + 0.29\left(\frac{T_s}{100}\right) \quad (10)$$

The G represents the incident radiation and q_{Rx} denotes as the net radiative heat flux in the flow direction. These quantities can be determined from the equation of radiative transfer. Once the radiation field is specified, the quantities G and q_{Rx} can be readily evaluated. The radiative heat equation of the present research is solved by the P_1 approximation (17) and is written as:

$$\frac{dq_{Rx}}{dx} + \left(1-\omega\right)\beta\left(G - 4\sigma T_s^4\right) = 0, \quad (11)$$

$$\frac{dG}{dx} + 3\left(1-\omega\tilde{g}\right)\beta q_{Rx} = 0. \quad (12)$$

The boundary conditions for (2), (3), (4), (11) and (12) are given as follows:

$$x = 0: \quad T_f = T_\infty, \ \frac{\partial T_s}{\partial x} = 0, \ G - 2q_{Rx} = 4\sigma T_\infty^4, \quad (13)$$

$$x = x_0: \quad \frac{\partial T_f}{\partial x} = \frac{\partial T_s}{\partial x} = 0, \ G + 2q_{Rx} = 4\sigma T_R^4. \quad (14)$$

3.2 Numerical Method

For convenience of calculations, the governing equations and associated boundary equations are transformed into dimensionless forms, and then the dimensionless equations are solved numerically using an implicit difference method. For solving the equation of transfer with the P_1 equations, and calculations of the T_f and T_s, the porous plate is divided into 300 equally spaced increments, whereas the optical thickness is divided into 600 equally spaced increments. To obtain the solutions of T_f and T_s, G or q_{Rx} are first determined based on an the assumption of temperature profile, and then the quantities of G and q_{Rx} are gained by solving equation of transfer or the P_1 equations at staggered lattice points (17). Once G is obtained, the finite difference equations for T_f and T_s can be solved readily by Gaussian elimination. Thereafter, the derived solutions of T_f and T_s are substituted into the equation of transfer or the P_1 equations and the energy equations to get new solutions of these quantities; similar calculations are repeated until the following convergence criterion is satisfied: $\left|\left(Q^{(n)} - Q^{(n-1)}\right)/Q^{(n)}\right| < 10^{-5}$. Here, Q represents T_f, T_s, G or q_{Rx}, and n is time interval of calculation. After obtaining the T_f, T_s and G, two efficiencies, temperature efficiency (η_T) and conversion efficiency (η_C) are evaluated as follows:

$$\eta_T = \frac{\left[T_R - \left(T_{s,x=0} - T_{s,x=x_0}\right)/2\right]}{T_R - T_\infty}, \quad (15)$$

$$\eta_C = \frac{\rho_f C_{Pf} u_f \left(T_{f,x=x_0} - T_{f,x=0}\right)}{q_{Rx,f}}. \quad (16)$$

The physical meaning of η_T is the indicating how close the mean temperature of a porous heat plate to that of inlet air and η_C is regarded as the ability of porous material in transferring energy by convection after absorbed from heat radiation,

4. Experimental Apparatus and Procedure

4.1 Experimental Apparatus

Figure 2 shows a schematic diagram of the present experimental apparatus. The experimental set-up was constructed similar to that of Kamiuto et al. (14),

but the double-tube heat exchanger was installed at the air inlet to keep air temperature at 25 – 30 ^{o}C when it reached the back surface of the porous plate. Therefore, the present transpiration cooling system consisted of 4 sections including heat exchanger, inlet air, porous medium, and radiation section. Air from a blower that was used as the transpiration gas was blown through the heat-exchanger and measured the flow rate using a rotameter. The air was then flowed upward through a stainless pipe (0.01 m inner diameter and 0.6 m high) instead of acrylic pipe as in Kamiuto et al. (14). A porous plate made of Alumina-Cordierite (Al-Co) was placed on the top of the stainless pipe. The physical characteristics of the examined porous plate were summarized in table 1. Four 250-W infrared lamps were aligned above the porous plate to irradiate the heat into the upper surface of the plate. The amount of radiant energy was measured using heat flux sensor manufactured by Hukesflux Thermal Sensor, model HFP01-05. The intensity of the infrared lamps was regulated manually from 50 V to 250 V; thus the radiative heat flux was varied from 0.97 to 16.59 kW/m^2.

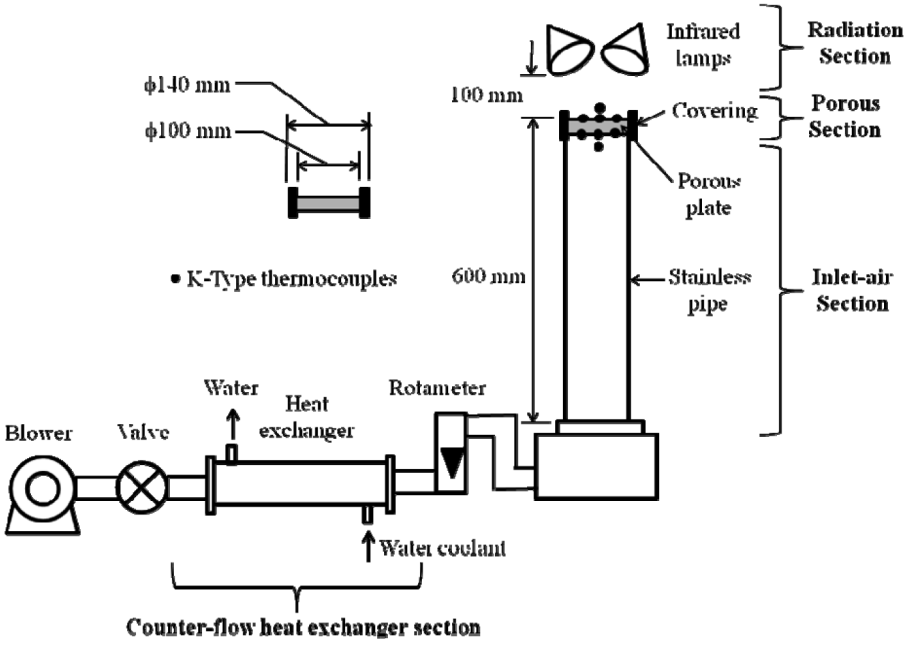

Figure 2. Schematic diagram of the experimental apparatus.

Table 1. Physical characteristics of a Alumina-Cordierite (Al-Co) open-cellular porous material

Coefficients		Quantities
Porosity	ϕ	0.875
Pores per inches	PPI	20
Thickness	x	0.0103 m
Extinction coefficient	β	365.89 m^{-1}
Optical thickness	τ	3.77

4.2 Experimental Procedure

The procedure of the experimental operation of the present cooling system is also similar to those of Kamiuto et al. (14). After the infrared lamps are switched on, it takes about 40 - 60 minutes to attain a steady-state of the temperatures of the porous plate. Six type-K thermocouple elements of 0.0003 m in diameter are adhered on the upper and lower surfaces of the porous plate by dividing as three for each surface. Inlet and outlet air temperature are measured using type-K sheathed thermocouple. The air velocity is varied from 0.364 - 1.274 m/s.

5. Results and Discussion

5.1 Effects of Air Flow Velocity (u_f) on Temperature Profile

Figure 3 presented the theoretical results of the temperature profiles of the solid (T_s) and the gas phases (T_f) inside the Al-Co porous plate, under the condition of irradiated heat flux $q_{Rx,f}$ = 12.48 kW/m^2. As seen first in Fig. 3 (a), the measured mean surface temperatures of the front and back porous plate are indicated by symbols, while the calculated results for the solid phase (T_s) is presented using the lines. The trend of T_s increased along the porous length because the incident radiation from the infrared lamps was emitted down to the front surface. For a fixed position of the thickness (x), the temperature profiles of T_f deceased as the air velocity (u_f) increased owing to the effects of a higher convective heat transfer (10). Agreement between the prediction calculated by basing on the P_1 equation in the radiative transfer equation (RTE) and the experimental results at the back (x = 0 mm) and the front surface (x = 10 mm) were satisfactory. In Fig. 3 (b), the temperature profiles of T_f showed the trend similar to T_s case; it increased along the porous length and deceased with u_f increasing. For comparison of T_s and T_f, it was obviously found that T_s was higher than T_f because the solid porous phase received the radiation heat flux directly and then, next step, the energy absorbed by porous material was transferred to the air supplied into system (18).

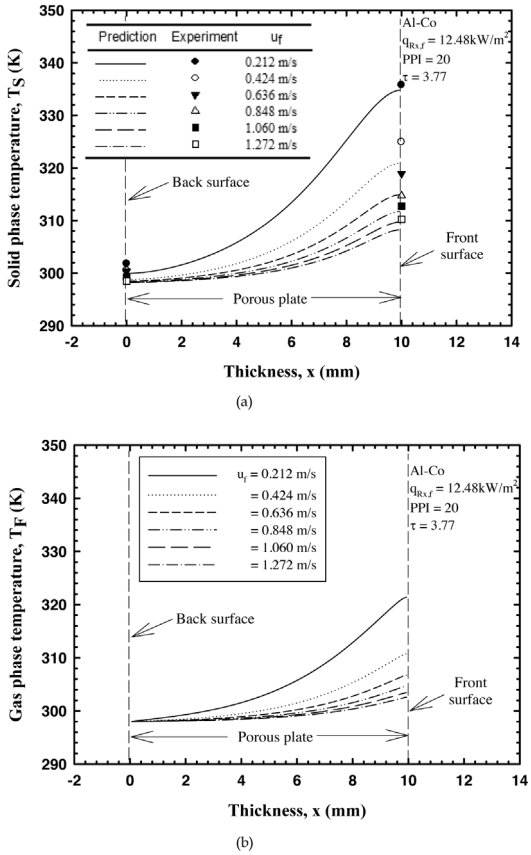

Figure 3. Profiles of T_s and T_f within the Al-Co open-cellular plate for the effect of u_f

5.2 Effects of Heat Flux on Temperature Profile

Figure 4 showed the theoretical results of the temperature profile of the solid (T_s) and the gas phases (T_f) inside the Al-Co porous plate, under the condition of air flow velocity (u_f) of 0.848 m/s. As seen first in Fig. 4 (a), the trend of T_s increased along the porous length due to incident radiation from the infrared lamps. For a fixed position of thickness x, the temperature profiles

of T_s increased with radiative heat flux ($q_{Rx,f}$) owing to porous medium absorbed a higher radiant energy from the infrared lamps. Agreement between the prediction based on the P_1 model of RTE and the experimental results at the back (x = 0 mm) and the front surface (x = 10 mm) were satisfactory. In Fig. 4 (b), the temperature profiles of T_f expressed the trend similar to T_s case; it increased along the porous length gradually and increased with $q_{Rx,f}$. For comparison of T_s and T_f, it was obviously found that T_s was higher than T_f which was described by the same reason of Fig. 3 (b).

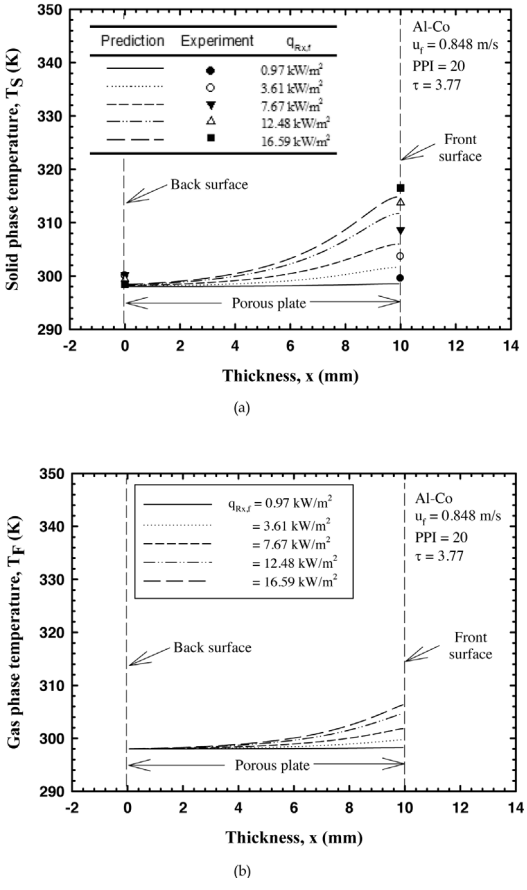

Figure 4. Profiles of T_s and T_f within the Al-Co open-cellular plate for the effect of $q_{Rx,f}$

5.3 The Temperature Efficiency (η_T)

Figure 5 shows variations in the temperature efficiency η_T against Reynols number (Re). In this study, Re represents the air flow velocity which is defined by using $\rho_f u_f D_s/\mu_f$, where μ_f is viscosity of a gas phase (Pa•s), and D_s is the equivalent strut diameter (m) as described in Krittacom (15). The experimental results are shown using symbols, while the numerical results are indicated by using the lines. The figure depicted that the η_T increased rapidly with Re and then asymptotic to a constant value for the Re higher than 15. However, at a fixed Re, the η_T decreased with the increase of the incident radiation due to a higher difference of an average temperature of porous plate and air temperature fed to system was obtained. For the Re higher than 15, the values of η_T were greater than 95 percentage. This indicated that the average temperature of the porous plate was very close to the average heat shield temperature and inlet air temperature. Agreement between theory and experiment was acceptable which indicated the validity of the present numerical model.

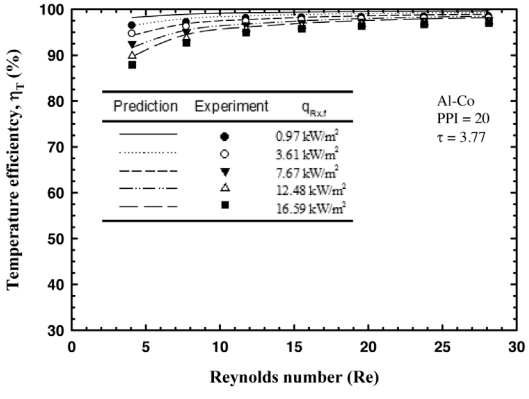

Figure 5. Temperature efficiency (η_T) of the Al-Co open-cellular porous plate

5.4 The Conversion Efficiency (η_C)

Figure 6 shows variations in the conversion efficiency η_C against Re. The results demonstrated that the η_C increased slightly with Re in which the η_C values were varied in the range of 40% to 60%. But the value of η_C was asymptotic to a constant value for the Re higher than 15. For a fixed value of Re, η_C

increased with incident radiation ($q_{Rx,f}$) because the porous media absorbed energy from a higher heat flux and then transferred via convection through the cooled-air flow. Thus, the ability of transferring energy of Al-Co open-cellular porous plate by convection after absorbing heat radiation decreased with the increasing of heat flux. Agreement between theory and experiment was acceptable.

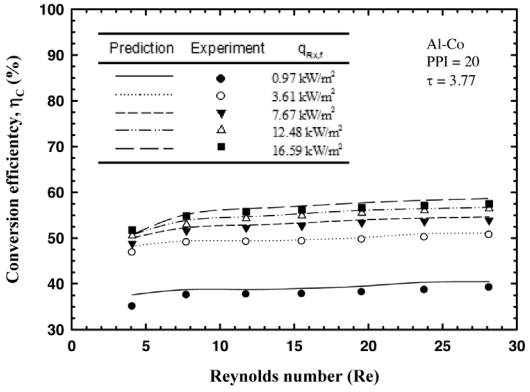

Figure 6. Conversion efficiency (η_C) of the Al-Co open-cellular porous plate

6. Conclusion

The major conclusions that can be drawn from the present study are summarized as follows:

1) The temperature profiles of gas (T_f) and solid (T_s) phase deceased as air injection velocity (u_f) increased because of the effects of a higher convective heat transfer, whereas the profiles of both temperature increased with incident radiation ($q_{Rx,f}$) owing to the effects of higher radiant energy.

2) The temperature efficiency (η_T) increased rapidly with Re and then asymptotic to a constant value for the Re higher than 15 but the η_T decreased with the increase of the $q_{Rx,f}$.

3) The conversion efficiency (η_C) of a Al-Co open-celled foam increased slightly with Re and and then asymptotic to a constant value for the Re higher than 15 as well as the value of η_C was governed by heat flux ($q_{Rx,f}$).

4) Agreement between the predicted results based on P_1 equations and experimental data was acceptable, thereby the validity of theoretical model was confirmed.

Suggestions and a Designed Tip

Incoming radiation from a radiative environment can be almost completely protected as long as the Re of the open-cellular plate was about 15 or higher. As a result, the transpiration cooling system as used in the present open-cellular porous plate should be designed for the Re = 15.

7. Acknowledgement

We are grateful to the Rajamangala University of Technology Isan (RMUTI) for the research fund. We also express our thanks to Mr.Jeerasak Kamluang, Miss Pensiri Thikumrum, Mr.Kriengkai Dastaisong, Mr.Kritsada Poohbunya and Mr. Chutchai Krongpeug, students who is the members of the Development in Technology of Porous Materials Research Laboratory (DITO-Lab), for their assistance in performing some part of the experiments.

8. References

(1) Grootenhuis P. The mechanism and application of effusion cooling. Journal of the Royal Aeronautic Society. 1959; 63: pp. 73–89.

(2) Choi SH, Scotti SJ, Song KD and Ries H. Transpiring cooling of a scram-jet engine combustion chamber: NASA (US); 1997. 8 p. Report No.: NASA AIAAA-97-2576.

(3) Glass DE, Dilley AD and Kelly HN. Numerical analysis of convection/ transpiration cooling.

AIAA J Spacecraft Rockets. 2001; 38(1): 15–20.

(4) Bayley FJ and Turner AB. The heat transfer performance of porous gas turbine blades. Aeronautical Journal. 1968; 72: 1087–1094.

(5) Bayley FJ and Turner AB. Transpiration cooled turbines. Journal Proceeding of the Institution of Mechanical Engineering with turbine. 1970; 185(1): 943-956.

(6) Duwez P and Wheeler HL. Experimental study of cooling by injection of a fluid through a porous material. Journal of Aeronautical Sciences. 1948; 15: 509 – 521.

(7) Andrews GE and Asere A. Transpiration cooling of gas turbine combustion chamber walls. Institute of Chemical Engineering Symposium Series. 1984; 86: 1047-1056.

(8) Fu X, Viskanta R and Gore JP. Measurement and correlation of volumetric heat transfer coefficients. Experimental and Thermal and Fluid Science. 1988; 17(4): 285-293.

(9) Kubota H. Thermal response of a transpiration-cooled system in a radiative and convective Environment. Transaction of the ASME: Journal of Heat Transfer. 1977; 99: 628 – 633.

(10) Eckert ERG and Cho HH. Transition from transpiration to film cooling. Int J Heat Mass Transfer. 1994; 37 (suppl 1): 3–8.

(11) Wolfersdorf JV. Effect of coolant side heat transfer on transpiration. Heat Mass Transfer. 2005; 41:.327-337.

(12) Andoh YH and Lips B. Prediction of porous walls thermal protection by effusion or transpiration cooling. An analytical approach. Applied Thermal Energy. 2003; 23(15): 1947-1958.

(13) Jiang P-X, Yu L, Sun J-G and Wang J. Experimental and numerical investigation of convection heat transfer in transpiration cooling. Applied Thermal Engineering. 2004; 24 (8-9): 1271-1289.

(14) Kamiuto K. Thermal characteristics of transpiration cooling system using open-cellular porous materials in a radiative environment. 2005; 7: 58-96.

(15) Ogushi T, Chiba H, Tane M and Nakajima H. Cellular and Porous Materials. Ochsner A, Murch GE and Lemon M JS, editor. Wiley-VCH Verlag GmbH & Co. KGaA; 2008.

(16) Krittacom B. Studies on Thermal Characteristics of Open-Cellular Porous Burners [Ph.D. Thesis]. Oita, Japan: Oita University; 2009.

(17) Kamiuto K, Saito S and Ito K. Numerical model for combined conductive and radiative heat transfer in annular packed beds. Numerical Heat Transfer, Part A. 1993; 23: 433-443.

(18) Krittacom B and Amatachaya P. Comparison of radiative heat transfer equation in porous materials solving by the equation of formal solution and the P_1 approximation equation. Engineering Journal of Siam University. 2008; 9(1): 20-30. Thai.